

## Excited Singlet ( $S_1$ ) State Resonance Raman Analysis of $N,N,N',N'$ -Tetramethylbenzidine and $N,N,N',N'$ -Tetramethyl-*p*-phenylenediamine

Laurent Boilet, Guy Buntinx, Christophe Lefumeux, and Olivier Poizat\*

Laboratoire de Spectrochimie Infrarouge et Raman (UMR 8516 de l'Université et du CNRS), Centre d'Etudes et de Recherches Lasers et Applications (FR 2416 du CNRS), Bât. C5, Université des Sciences et Technologies de Lille, 59655 Villeneuve d'Ascq, France

Received: June 2, 2003

Vibrational data on the first excited singlet state ( $S_1$ ) of  $N,N,N',N'$ -tetramethylbenzidine (TMB) and  $N,N,N',N'$ -tetramethyl-*p*-phenylenediamine (TMPD) have been obtained by using picosecond time-resolved Raman spectroscopy for different isotopic derivatives and for the  $N,N,N',N'$ -tetraethyl analogues, TEB and TEPD. Reliable vibrational assignments are proposed. On this basis, the  $S_1$  state structure and electronic configuration of these diamines are discussed and compared with the results previously reported for the ground state, the lowest excited triplet state, and the radical cation species.

### 1. Introduction

Aromatic diamines such as  $N,N,N',N'$ -tetramethyl-*p*-phenylenediamine (TMPD) and  $N,N,N',N'$ -tetramethylbenzidine (TMB) are easily photoionized in polar solvents because of their low ionization potential. The reaction occurs via a monophotonic process from the fluorescent state  $S_1$ . These molecules have thus been used as model compounds for studying the mechanism of electron photoejection and solvation.<sup>1–16</sup> Kinetic data from transient absorption, emission and photoconductivity measurements strongly suggest that specific interactions between the solvent and excited solute molecules play an important role in the ionization process.<sup>7–15</sup> The charge separation is shown to result from electron transfer from the excited solute to a solvent cluster with configuration depending on the solvent nature. Obtaining structural information on these transient species as a function of the solvent would complement advantageously the present knowledge about the dynamics of photoionization. In this respect, time-resolved vibrational spectroscopy is able to provide detailed information on the structure and conformation of chemical intermediates. Several vibrational analyses of the radical cation of TMPD based on time-resolved resonance Raman experiments<sup>17,18</sup> and on ab initio calculations<sup>19</sup> have been reported. The radical cation of TMB has also been the object of time-resolved resonance Raman<sup>20</sup> and ab initio<sup>21</sup> studies. Similarly, the lowest excited triplet state of TMPD<sup>17,18,22,23</sup> and TMB<sup>24</sup> has been investigated by time-resolved resonance Raman spectroscopy.

We are now interested by the TMPD and TMB lowest excited singlet state  $S_1$  responsible for the monophotonic ionization. A brief discussion of time-resolved resonance Raman spectra of  $S_1$  TMPD has been previously reported.<sup>25</sup> However, this investigation was limited to a very narrow spectral range (1100–1600  $\text{cm}^{-1}$ ). In this paper, we present a comprehensive analysis of the  $S_1$  state time-resolved resonance Raman spectra obtained for four isotopomers of the TMPD and TMB diamines: the fully hydrogenated and ring- or methyl-deuterated or both derivatives. The fully hydrogenated and ring-deuterated deriva-

tives of the tetraethyl analogues TEPD and TEB are also studied. The designation used in the following for all species is given in Table 1. The vibrational assignment will be established by analogy with the rigorous description of the normal modes of vibration in terms of potential energy distributions (PEDs) previously obtained from ab initio calculations for the TMPD radical cation<sup>19</sup> and the TMB ground-state  $S_0$  and radical cation.<sup>21</sup> In fact, in such aromatic systems where the normal modes are distributed on a large number of internal coordinates, the PEDs are not expected to be significantly modified upon electronic excitation or ionization. This assumption is confirmed by the observation that the vibrational frequency shifts induced by isotopic substitution remain nearly similar in all cases. On this basis, the  $S_1$  state vibrational assignment and structure of TMPD and TMB will be discussed and compared with the analogous data reported for the ground state, triplet state, and radical cation of these molecules.

### 2. Experimental Section

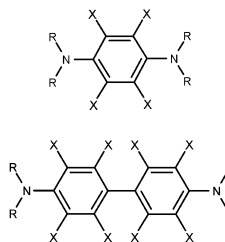
TMB and TMPD were purchased from Aldrich. The different deuterated derivatives were synthesized as reported elsewhere.<sup>26</sup> All samples were sublimed in vacuo prior to each spectroscopic measurement. Hexane, acetonitrile, and methanol (SDS, spectroscopic grade) were used as received. Aqueous solutions were made with distilled and deionized water. All measurements were performed on  $10^{-3}$  M solutions.

The picosecond Raman scattering experimental setup has already been described.<sup>27–28</sup> Briefly, it comprises a 1 kHz Ti:sapphire laser system based upon a Coherent (MIRA 900D) oscillator and a BM Industries (ALPHA 1000) regenerative amplifier. The laser source was set in a picosecond configuration. The output wavelength was set at 752 nm for the probe excitation ( $\sim 0.6 \mu\text{J}$ , 2.4 mJ/cm per pulse). Pump pulses at 250.6 nm ( $\sim 15 \mu\text{J}$ ) were obtained by tripling the 752-nm fundamental. The pump–probe cross correlation fwhm was  $\sim 4$  ps. The pump–probe polarization configuration was set at the magic angle. Scattered light was collected at  $90^\circ$  to the incident excitation and sent through a Notch filter into a home-built polychromator coupled to a CCD camera (Princeton Instrument LN/CCD-1100-PB-UV/AR detector + ST-138 controller). The

\* To whom correspondence should be addressed. Fax: +33-320336354. E-mail: poizat@univ-lille1.fr.

TABLE 1: Nomenclature of the Investigated Amines

X	R = CH <sub>3</sub>	R = CD <sub>3</sub>	R = C <sub>2</sub> H <sub>5</sub>
H	TMPD- <i>h</i> <sub>16</sub>	TMPD- <i>d</i> <sub>12</sub>	TEPD- <i>h</i>
D	TMPD- <i>d</i> <sub>4</sub>	TMPD- <i>d</i> <sub>16</sub>	TEPD- <i>d</i> <sub>4</sub>
H	TMB- <i>h</i> <sub>20</sub>	TMB- <i>d</i> <sub>12</sub>	TEB- <i>h</i>
D	TMB- <i>d</i> <sub>8</sub>	TMB- <i>d</i> <sub>20</sub>	TEB- <i>d</i> <sub>8</sub>



flowing jet sampling technique was adopted (1 mm diameter jet). The wavenumber shift was calibrated using the Raman spectrum of indene. Data collection times were  $\sim 10$  min.

### 3. Results and Discussion

For both the TMB and TMPD amines, the experimental S<sub>1</sub> state Raman spectra were recorded in resonance with strongly allowed electronic transitions, and thus, the vibrational activity was assumed to have essentially a Franck–Condon origin. Consequently, only the totally symmetric modes are expected to be active in the Raman spectra. In the text below, the normal modes of vibration of the phenyl rings are labeled according to the convention used by Varsanyi for para-disubstituted benzenes,<sup>29</sup> adapted from the Wilson notation for benzene.<sup>30</sup>

**3.1. TMB S<sub>1</sub> State. Vibrational Spectra and Assignments.** The TMB S<sub>1</sub> state was produced by photoexcitation at 250.6 nm within a strong S<sub>0</sub>  $\rightarrow$  S<sub>n</sub> absorption band,<sup>11</sup> followed by ultrafast internal conversion. This species presents two strong absorption bands in the visible region, a sharp one centered at 450 nm and a broader one extending from 700 to 1000 nm with a maximum around 900 nm.<sup>9–10</sup> The 752-nm probe excitation used in this work was in resonance with the latter transition. No spectrum could be obtained in resonance with the 450 nm band due to an intense fluorescence emission. A 100 ps pump–probe delay was chosen, which is much shorter than the 10 ns lifetime of the S<sub>1</sub> state of TMB in *n*-hexane.<sup>11</sup> The TMB radical cation and singlet state, having similar absorption spectra, both led to enhanced resonance Raman spectra at 752 nm. To avoid the production of the radical cation, measurements were made in *n*-hexane, in which no monophotonic ionization of TMB occurs, and a low pump intensity was used to reduce the biphotonic ionization. Spectra recorded in these conditions for the different TMB and TEB isotopomers (region 1800–600 cm<sup>−1</sup>) are presented in Figure 1. The 200–600 cm<sup>−1</sup> frequency domain has also been probed, but no Raman signal could be detected in this range. For each spectrum, the solvent signal, recorded separately in the absence of pump excitation, has been subtracted after normalization. An artifact of subtraction is apparent around 900 cm<sup>−1</sup> (symbol S in Figure 1). A series of measurements made for different intensities of the pump excitation indicate that a weak band around 1600 cm<sup>−1</sup> (symbol R in Figure 1) is due to the most intense peak (mode 8a<sup>21</sup>) of the radical cation species produced via biphotonic ionization. The frequency shifts are consistent with those reported previously.<sup>21</sup> All of the other Raman bands observed in these spectra can be ascribed to the S<sub>1</sub> state. As a confirmation, the same bands were detected in polar solvents (methanol, acetonitrile), in addition to the strong spectrum of the radical cation produced monophotonically.

As stated above, only the totally symmetric modes are expected to be active in the S<sub>1</sub> state resonance Raman spectra

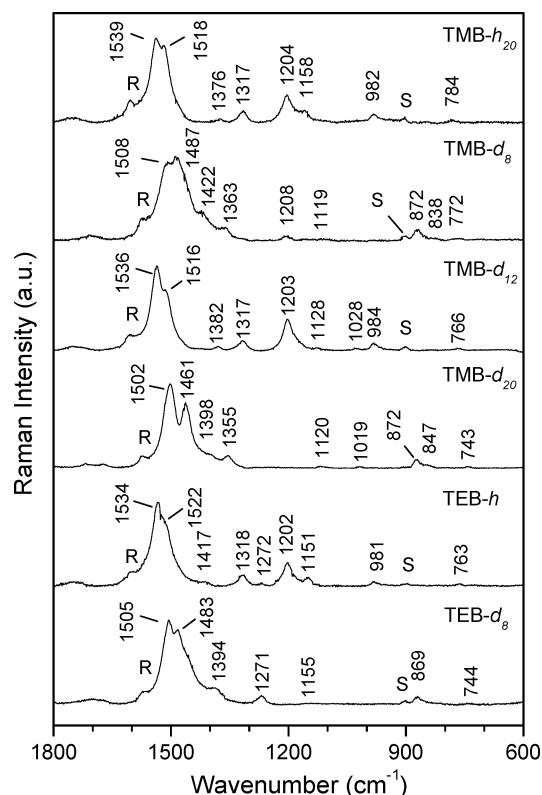


**Figure 1.** Time-resolved resonance Raman spectra (600–1800 cm<sup>−1</sup>) of the TMB and TEB isotopomers in the first excited (S<sub>1</sub>) state obtained upon 752 nm probe excitation 100 ps after pump excitation at 250.6 nm. Solvent bands (*n*-hexane) have been subtracted. The main band frequencies (cm<sup>−1</sup>) are given. Symbol “S” indicates an artifact due to a bad subtraction of a strong solvent band. Symbol “R” indicates signals due to the radical cation.

of TMB. The highest possible symmetry corresponds to a D<sub>2h</sub> planar NC<sub>2</sub>–C<sub>6</sub>H<sub>4</sub>–C<sub>6</sub>H<sub>4</sub>–NC<sub>2</sub> skeleton, as for the radical cation<sup>21</sup> and T<sub>1</sub> state.<sup>24</sup> In this hypothesis, 14 A<sub>g</sub> modes are expected for TMB between 1800 and 200 cm<sup>−1</sup>: the inter-ring stretch ( $\nu_{ir}$ ) and the in-phase combination of the N-ring bond stretches ( $\nu_{N-ring}^s$ ), seven in-plane ring motions (8a, 19a, 9a, 18a, 1, 12, and 6a), and five modes of the N(CH<sub>3</sub>)<sub>2</sub> groups (2 CH<sub>3</sub> bendings, 1 CH<sub>3</sub> rocking, the symmetric combination of the N–CH<sub>3</sub> stretches,  $\nu^s$ (NC<sub>2</sub>), and the symmetric CH<sub>3</sub>–N–CH<sub>3</sub> in-plane distortion,  $\Delta^s$ (NC<sub>2</sub>)). If the structure presents an inter-ring twist (D<sub>2</sub> symmetry for the NC<sub>2</sub>–C<sub>6</sub>H<sub>4</sub>–C<sub>6</sub>H<sub>4</sub>–NC<sub>2</sub> skeleton) as in the ground state,<sup>21</sup> five additional modes become totally symmetric: three out-of-plane ring vibrations, a CH<sub>3</sub> bending, and a CH<sub>3</sub> rocking.

The assignment of the observed S<sub>1</sub> state Raman bands of TMB (see Table 2) is established by comparing the frequencies and frequency shifts induced by isotopic substitution with those previously found for the ground state and the radical cation.

**TABLE 2:  $S_1$  State Raman Frequencies ( $\text{cm}^{-1}$ ) and Assignments (Wilson Notation) for the TMB and TEB Isotopic Derivatives**

TMB				TEB		assignment <sup>a</sup>
$-h_{20}$	$-d_8$	$-d_{12}$	$-d_{20}$	$-h$	$-d_8$	
1539	1508	1536	1502	1534	1505	8a
1518	1487	1516	1461	1522	1483	19a
	1422	1128	1120			$\delta(\text{CH}_3)$
1376	1363	1382	1355	1417	1394	$\nu_{\text{N-ring}}^s$
1317	1208	1317		1318		$\nu_{\text{ir}}$
1204	872	1203	872	1202	869	9a
				1272	1271	$\delta(\text{CH}_2)$
1158	1119	1028	1019	1151	1155	$\rho(\text{CH}_3)$
982	838	984	847	981		18a
784	772	766	743	763	744	1

<sup>a</sup>  $\delta$  = in-plane deformation,  $\nu$  = stretching,  $\rho$  = rocking.

Some bands of which the frequency is only sensitive to deuteration of the phenyl rings can be easily ascribed to typical vibrations of the phenyl rings: in the  $-h_{20}$  and  $-d_8$  spectra, mode 8a (in-plane CC stretch) is unambiguously located at 1539 and 1508  $\text{cm}^{-1}$ , respectively, mode 9a (CCH in-plane bending) at 1204 and 872  $\text{cm}^{-1}$ , and mode 18a (mixed in-plane CCH bending and ring deformation) at 982 and 838  $\text{cm}^{-1}$ . Nearly similar isotopic shifts were observed for the ground state and the radical cation.<sup>21</sup> The 1317- $\text{cm}^{-1}$  band is insensitive to deuteration of the methyl groups but seems to disappear by ring deuteration. We associate it with that observed at 1208  $\text{cm}^{-1}$  in the  $-d_8$  derivative and ascribe it to the inter-ring stretching mode,  $\nu_{\text{ir}}$ . The corresponding frequency shift is the same as that noticed for the radical cation. The band intensity decrease noted for this mode upon ring deuteration (it even completely disappears in the  $-d_{20}$  derivative) has been observed similarly in the radical cation spectra and correlated to a potential energy redistribution effect typical of the biphenyl derivatives<sup>21</sup> (decrease of the contribution of the inter-ring stretching coordinate). The very weak band at 1376  $\text{cm}^{-1}$  is attributed to the  $\nu_{\text{N-ring}}^s$  stretching mode as it undergoes unusual frequency shifts, analogous to those observed for this mode in the ground state: slight frequency decrease upon ring deuteration (1363  $\text{cm}^{-1}$  in TMB- $d_8$ ), slight frequency increase upon methyl deuteration (1382  $\text{cm}^{-1}$  in TMB- $d_{12}$ ), and more significant increase by substitution of the methyl by ethyl groups (1417  $\text{cm}^{-1}$  in TEB- $h$ ). This complex behavior can be explained as resulting from the different couplings of the N-ring stretch with the  $\text{CH}_3$ ,  $\text{CD}_3$ , and  $\text{C}_2\text{H}_5$  internal vibrations. The intense band at 1518  $\text{cm}^{-1}$  is shifted to 1516  $\text{cm}^{-1}$  (TMB- $d_{12}$ ), 1487  $\text{cm}^{-1}$  (TMB- $d_8$ ) and 1461  $\text{cm}^{-1}$  (TMB- $d_{20}$ ). By analogy with the ground-state TMB spectra in which the same frequency shifts were observed, we assign this band to the ring mode 19a. The very weak signal at 784  $\text{cm}^{-1}$  undergoes slight shifts by ring deuteration (772  $\text{cm}^{-1}$ ) and methyl deuteration (766  $\text{cm}^{-1}$ ) that are characteristics of the in-plane ring mode 1. By analogy with the ground state and radical cation assignments, we associate the band at 1158  $\text{cm}^{-1}$  in the perhydrogenated derivative with those lying at 1119, 1028, and 1019  $\text{cm}^{-1}$  in the  $-d_8$ ,  $-d_{12}$ , and  $-d_{20}$  derivatives, respectively, and assign it to a  $\rho(\text{CH}_3)$  mode. Similarly, a line at 1272  $\text{cm}^{-1}$  only visible in the spectra of the TEB derivatives is ascribed to a typical bending of the  $\text{CH}_2$  group. The assignment of the remaining bands is more doubtful. By analogy with the radical cation, the bands at 1422 (TMB- $d_8$ ), 1128 (TMB- $d_{12}$ ), and 1120  $\text{cm}^{-1}$  (TMB- $d_{20}$ ) could be assigned to a  $\delta(\text{CH}_3)$  mode located at 1446 and 1431  $\text{cm}^{-1}$  in the TMB- $d_8$  ground state and radical cation Raman spectra, respectively. A very weak signal at 1398  $\text{cm}^{-1}$  in the TMB- $d_{20}$  spectrum remains unassigned.

**TABLE 3: Comparison of Some Characteristic Frequencies ( $\text{cm}^{-1}$ ) for the Ground State ( $S_0$ ),<sup>a</sup> the Radical Cation ( $R^+$ ),<sup>a</sup> and the Excited Triplet ( $T_1$ )<sup>b</sup> and Singlet ( $S_1$ ) States of TMB- $h_{20}$** 

normal mode	$S_0$ <sup>a</sup>	$R^+$ <sup>a</sup>	$T_1$ <sup>b</sup>	$S_1$
8a	1604	1603	1593	1539
19a	1539	1558	1508	1518
$\nu_{\text{N-ring}}^s$	1359	1402	1380	1376
$\nu_{\text{ir}}$	1288	1342	1360	1317

<sup>a</sup> From ref 21. <sup>b</sup> From ref 24.

**Structural Implications.** All assignments in Table 2 were established by transfer from those determined with certainty for the ground state and the radical cation. Their validity is guaranteed by the similarity of the isotopic frequency shifts observed in these three states. The nine bands detected for the  $S_1$  state of TMB (10 in the case of TEB) correspond unambiguously to some of the totally symmetric modes expected in the assumption of a  $D_{2h}$  symmetry. The resonance Raman activity and, to a lesser extent, the relative intensities are close to those observed in the radical cation spectrum probed at the same wavelength (see Figure 4 in ref 21). No band splitting is observed, attesting to the equivalence of the two anilino moieties, and no spectral indication of an out-of-plane distortion (activity of out-of-plane modes) is discernible. All of these results strongly suggest that the  $\text{NC}_2\text{-C}_6\text{H}_4\text{-C}_6\text{H}_4\text{-NC}_2$  skeleton adopts a planar  $D_{2h}$  conformation in the excited  $S_1$  state, as in the radical cation.

Let us compare in more detail the frequency of four vibrational modes of the TMB ground state,<sup>21</sup> radical cation,<sup>21</sup> and first excited triplet<sup>24</sup> and singlet states that are especially sensitive to changes in the electronic configuration (Table 3). These are the typical ring vibrations 8a and 19a and the key bridging bond stretches,  $\nu_{\text{ir}}$  and  $\nu_{\text{N-ring}}^s$ . The radical cation of TMB is essentially characterized by the strong increase of the  $\nu_{\text{ir}}$  and  $\nu_{\text{N-ring}}^s$  frequencies relative to the ground-state values (+43 and +54  $\text{cm}^{-1}$ , respectively). These shifts were correlated to an intensification of the  $\pi$  character of these bonds due to the appearance of a quinoidal distortion.<sup>21</sup> The weaker increase in frequency of mode 19a (+19  $\text{cm}^{-1}$ ) can be explained similarly as its PED contains an important contribution of the N-ring coordinate. The same kind of quinoidal distortion is observed in the triplet state with a considerable strengthening of the inter-ring bond ( $\Delta\nu_{\text{N-ring}}^s = +21$   $\text{cm}^{-1}$  and  $\Delta\nu_{\text{ir}} = +72$   $\text{cm}^{-1}$ ). The slight decrease in frequency noticed for modes 8a and 19a on going from the ground state to the triplet state reflects the lowering of the  $\pi$ -bonding in the rings due to the presence of an electron in a  $\pi^*$  orbital.

In contrast to the  $T_1$  state, the  $S_1$  state is rather characterized by an important decrease in frequency of mode 8a ( $\Delta\nu = -65$   $\text{cm}^{-1}$ ), whereas the  $\nu_{\text{ir}}$  and  $\nu_{\text{N-ring}}^s$  frequencies are only weakly increased relative to the ground-state value (+29  $\text{cm}^{-1}$  and +17  $\text{cm}^{-1}$ , respectively). These results indicate that the antibonding density ( $\pi^*$  charge) is much more confined in the phenyl rings in the case of the  $S_1$  state than of the  $T_1$  state.

In conclusion, this analysis suggests that no significant quinoidal distortion occurs in the  $S_1$  state of TMB, the electronic perturbation being essentially localized on the rings, whereas in the radical cation and the triplet state the perturbation is rather delocalized on the entire molecule through the N-ring and inter-ring bonds. Despite this difference, a planar configuration ( $D_{2h}$ ) of  $S_1$  is probable, as for the  $T_1$  state and radical cation species.

**3.2. TMPD  $S_1$  State. Vibrational Spectra and Assignments.** The TMPD  $S_1$  state was produced by photoexcitation at 250.6



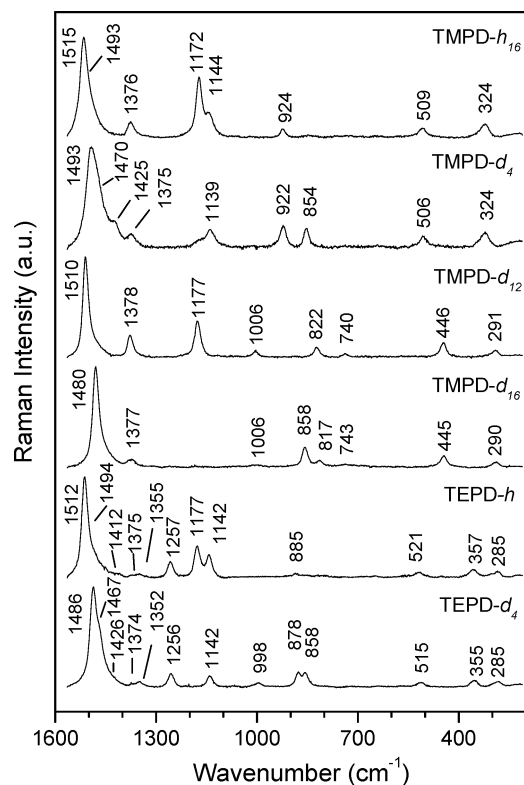


**Figure 2.** Time-resolved resonance Raman spectra (600–1800 cm<sup>-1</sup>) of the TMPD and TEPD isotopomers in the first excited (S<sub>1</sub>) state obtained upon 752 nm probe excitation 30 ps after pump excitation at 250.6 nm. Solvent bands (methanol) have been subtracted. The main band frequencies (cm<sup>-1</sup>) are given.

nm in resonance with a strong absorption band of S<sub>0</sub> TMPD.<sup>31</sup> The 752 nm probe excitation was in resonance with a strong S<sub>1</sub> → S<sub>n</sub> absorption band lying between 500 and 800 nm.<sup>31</sup> In contrast, the TMPD radical cation absorption (450–650 nm) was completely out of resonance at this wavelength, and thus, pure S<sub>1</sub> state resonance Raman spectra could be readily obtained. All spectra were recorded 30 ps after photoexcitation. Similar spectra were obtained in *n*-hexane, methanol, acetonitrile, and water, which indicates that the S<sub>1</sub> structure is identical in all cases. Figure 2 shows the time-resolved resonance Raman spectra of the different TMPD and TEPD isotopic derivatives recorded in the spectral range 1600–200 cm<sup>-1</sup> in methanol. Concerning the most intense bands, these spectra are comparable with those obtained by Takahashi et al. for the spectral region 1100–1600 cm<sup>-1</sup> by nanosecond pump and probe excitations at a delay of 0 ns.<sup>25</sup> However, new weak lines are observed in the present investigation, in particular, the 1376 cm<sup>-1</sup> in the TMPD-*h*<sub>16</sub> spectrum. In Figure 3 are compared the resonance Raman spectra of the excited S<sub>1</sub> state (probed at 752 nm), excited T<sub>1</sub> state (probed at 610 nm),<sup>18</sup> and radical cation (probed at 647 nm)<sup>18</sup> of TMPD-*h*<sub>16</sub>. An evident analogy is observed between these three spectra concerning both the resonance Raman activity and relative intensities: nearly the same number of bands are detected in each spectral region (three lines above 1400 cm<sup>-1</sup>, two neighboring lines around 1200 cm<sup>-1</sup>, and three weak signals at about 930, 510, and 320 cm<sup>-1</sup>, respectively). It is thus reasonable to assume that the S<sub>1</sub> state structure adopts the same planar D<sub>2h</sub> symmetry of the NC<sub>2</sub>–C<sub>6</sub>H<sub>4</sub>–NC<sub>2</sub> skeleton as that previously established for the triplet state and the radical cation species.<sup>18–19</sup> In this hypothesis, seven totally symmetric modes of the NC<sub>2</sub>–C<sub>6</sub>H<sub>4</sub>–NC<sub>2</sub> skeleton (four ring modes, 8a, 1, 6a, and 9a, and three modes for the NC<sub>2</sub> groups, ν<sup>s</sup><sub>N–ring</sub>,

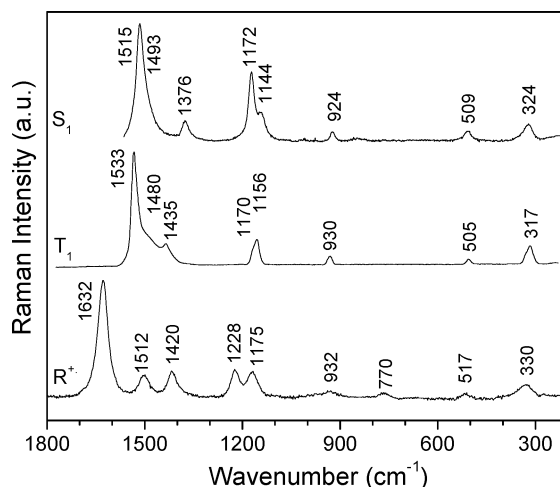


**Figure 3.** Time-resolved resonance Raman spectra of the S<sub>1</sub> state (probed at 752 nm), T<sub>1</sub> state (probed at 610 nm, from ref 18), and the radical cation R<sup>•+</sup> (probed at 647 nm, from ref 18) of TMPD-*h*<sub>16</sub>.

ν<sup>s</sup>(NC<sub>2</sub>), and Δ<sup>s</sup>(NC<sub>2</sub>)), plus three methyl vibrations (two CH<sub>3</sub> bendings, one CH<sub>3</sub> rocking) are expected between 1800 and 200 cm<sup>-1</sup>.

The assignment proposed for the S<sub>1</sub> state Raman bands of TMPD is given in Table 4. It is naturally deduced from that established for the radical cation Raman spectra<sup>18</sup> and improved by Brouwer on the basis of DFT calculations.<sup>19</sup> A brief comment concerning two points in this last report is nevertheless necessary before going into the S<sub>1</sub> state analysis. On one hand, the Raman band observed at 932 cm<sup>-1</sup> in the radical cation of TMPD, previously ascribed to the ν<sup>s</sup>(NC<sub>2</sub>) stretching mode,<sup>18</sup> was reattributed to the ring breathing mode 1 by Brouwer.<sup>19</sup> However, although the normal mode PEDs were not given in this paper, this description seems questionable in regard to the experimental and calculated frequency shifts of this band upon deuteration (absence of negative shift on ring deuteration (+16 cm<sup>-1</sup>) and considerable downshift on methyl deuteration (−104 cm<sup>-1</sup>). Moreover, in the case of the TMB radical cation, a Raman line located at the same frequency (939 cm<sup>-1</sup>), characterized by similar isotopic shifts (+6 and −109 cm<sup>-1</sup> on ring and methyl deuteration, respectively), and showing comparable downshift on going from methyl to ethyl substituents (−32 cm<sup>-1</sup>)<sup>20</sup> has been correlated from DFT calculations to a mode having dominant ν<sup>s</sup>(NC<sub>2</sub>) character.<sup>21</sup> According to the graphical representation predicted for the 932 cm<sup>-1</sup> mode of the TMPD radical cation,<sup>19</sup> a coupled ν<sup>s</sup>(NC<sub>2</sub>) + 1 motion seems the most adequate description. On the other hand, the Raman bands observed at 517 and 330 cm<sup>-1</sup> have been designated by Brouwer as pure Δ<sup>s</sup>(NC<sub>2</sub>) and in-plane ring bending vibrations (Δ<sub>ring</sub>), respectively. However, according to the graphical representation of these modes<sup>19</sup> and to the fact that their frequencies are essentially shifted upon methyl deuteration, both of them are likely involving important contributions from the Δ(NC<sub>2</sub>) internal coordinate and seem better described as Δ<sup>s</sup>(NC<sub>2</sub>) + Δ<sub>ring</sub> modes. Indeed, as commonly encountered in substituted benzene derivatives, the ν<sub>ring</sub> (1) and Δ<sub>ring</sub> (6a) modes of benzene become strongly mixed with the ring-substituent stretches and the internal motion of the substituents in such a way that they are distributed throughout many normal modes. Note finally that the important frequency upshift (+45 cm<sup>-1</sup>) observed for the ν<sup>s</sup><sub>N–ring</sub> mode of the TMPD radical cation upon methyl deuteration,<sup>18</sup> notably underestimated by the DFT calculations, reveals the presence of a significant contribution of the δ(CH<sub>3</sub>) internal coordinate to the PED of this mode in the -*h*<sub>16</sub> and -*d*<sub>4</sub> isotopomers.

**TABLE 4:  $S_1$  State Raman Frequencies ( $\text{cm}^{-1}$ ) and Assignments (Wilson Notation) for the TMPD and TEPD Isotopic Derivatives**

TMPD				TEPD		assignment <sup>a</sup>
$-h_{16}$	$-d_4$	$-d_{12}$	$-d_{16}$	$-h$	$-d_4$	
1515	1493	1510	1480	1512	1486	8a
1493	1470			1494	1467	$\delta(\text{CH}_3)$
	1425			1412	1426	
1376	1375	1378	1377	1375	1374	$\nu_{\text{N-ring}}^s$
				1355	1352	$\delta(\text{CH}_2)$
				1257	1256	
1172	854	1177	858	1177	858	9a
1144	1139	1006	1006	1142	1142	$\rho(\text{CH}_3)$
					998	$\delta(\text{C}_2\text{H}_5)$
924	922	822	817	885	878	$\nu^s(\text{NC}_2) + \nu_{\text{ring}}(1)$
		740	743			$\Delta_{\text{ring}}(6a)$
509	506	446	445	521	515	$\Delta^s(\text{NC}_2) + \Delta_{\text{ring}}(6a) (+\Delta\text{C}_2\text{H}_5)$
				357	355	
324	324	291	290	285	285	

<sup>a</sup>  $\nu$  = stretching,  $\Delta$  = in-plane distortions,  $\rho$  = rocking.

**TABLE 5: Comparison of Some Characteristic Frequencies ( $\text{cm}^{-1}$ ) for the Ground State ( $S_0$ ),<sup>a</sup> the Radical Cation ( $R^+$ ),<sup>b</sup> and the Excited Triplet ( $T_1$ ) and Singlet ( $S_1$ ) States of the TMPD Isotopic Derivatives**

$S_0^a$			$R^{+b}$			$T_1^b$			$S_1$			assignment
$h_{16}$	$d_4$	$d_{12}$	$h_{16}$	$d_4$	$d_{12}$	$h_{16}$	$d_4$	$d_{12}$	$h_{16}$	$d_4$	$d_{12}$	
1623	1598	1622	1632	1610	1632	1533	1516	1490	1515	1493	1510	8a
1345	1343	1330	1420	1430	1465				1376	1375	1378	$\nu_{\text{N-ring}}^s$
1217	885	1222	1228	888	1233	1170	835	1160	1172	854	1177	9a

<sup>a</sup> From ref 26. <sup>b</sup> From ref 18.

Consider now the  $S_1$  state resonance Raman spectra in Figure 2. The comparison of the spectra of the different isotopomers shows clearly that only two strong bands of the TMPD- $h_{16}$  species at 1515 and 1172  $\text{cm}^{-1}$  (1512 and 1177  $\text{cm}^{-1}$  in TEPD- $h$ ) are sensitive to ring deuteration. They shift to 1493 and 854  $\text{cm}^{-1}$ , respectively, in TMPD- $d_4$  (1486 and 858  $\text{cm}^{-1}$  in TEPD- $d_4$ ). Similar isotopic shifts are observed between the TMPD- $d_{12}$  and TMPD- $d_{16}$  derivatives. These shifts (approximately similar to those observed for the ground state and the radical cation) are unambiguously characteristic of the in-plane ring stretching 8a and CCH bending 9a modes, respectively. A band located around 1375  $\text{cm}^{-1}$  in the spectra of all derivatives is ascribed to the  $\nu_{\text{N-ring}}^s$  mode by analogy with the ground-state spectra in which this mode is also insensitive to any deuteration. Most of the other bands are insensitive to ring deuteration but are displaced by alkyl deuteration. They contain thus notable contributions from the  $\text{N}(\text{alkyl})_2$  internal coordinates. In the low-frequency region, two bands at 509 and 324  $\text{cm}^{-1}$  (TMPD- $h_{16}$  spectrum) can be readily correlated to those observed at 517 and 330  $\text{cm}^{-1}$ , respectively, in the radical cation spectrum and at 505 and 317  $\text{cm}^{-1}$  in the triplet state spectrum (see Figure 3) and characterized by comparable shifts by deuteration. According to the assignment of the radical cation discussed above, they are ascribed to mixed ring and CNC in-plane distortions of the type  $\Delta^s(\text{NC}_2) + \Delta_{\text{ring}}(6a)$ . In the TEPD derivatives, the lowest frequency band appears split into two signals at 357 and 285  $\text{cm}^{-1}$ , probably due to the additional contribution of an internal motion of the  $\text{C}_2\text{H}_5$  group. By analogy with the radical cation, we assign the 924  $\text{cm}^{-1}$  line in the perhydrogenated derivative to the  $\nu^s(\text{NC}_2) + 1$  coupled vibration because similar isotopic shifts are observed in both cases. A shoulder superimposed to the 8a band in the spectra of the  $-h_{16}$  ( $\sim 1493$   $\text{cm}^{-1}$ ) and  $-d_4$  ( $\sim 1470$   $\text{cm}^{-1}$ ) compounds and a band lying at 1144 and 1139  $\text{cm}^{-1}$ , respectively, in these spectra are attributed to in-plane bend and rocking vibrations of the methyl groups. These modes are also active in the spectra of the TEPD- $h$  and TEPD- $d_4$

derivatives. In this case, several additional weak signals are likely due to  $\text{CH}_2$  deformation modes (see Table 4). Finally two weak lines located at 740 and 743  $\text{cm}^{-1}$  in the TMPD- $d_{12}$  and TMPD- $d_{16}$  spectra can be correlated to the ring deformation mode  $\Delta_{\text{ring}}$  (mainly 6a).

**Structural Implications.** The frequency of some characteristic modes of the TMPD ground state,<sup>26</sup> radical cation,<sup>18</sup> and excited singlet and triplet states<sup>18</sup> are presented in Table 5. Let us first consider the modes 8a and 9a, which are, according to the radical cation PEDs,<sup>21</sup> strictly located in the ring. The frequencies of these modes in the  $S_1$  state (1515 and 1172  $\text{cm}^{-1}$ ) are clearly lower than those found in the ground state ( $\Delta\nu = -108$  and  $-45$   $\text{cm}^{-1}$ , respectively) or in the radical cation ( $\Delta\nu = -117$  and  $-56$   $\text{cm}^{-1}$ , respectively). These strong frequency changes denote a significant release of the global bond strength in the ring skeleton on excitation to  $S_1$ , in agreement with the appearance of a notable  $\pi^*$  charge. About similar frequency shifts arise in the triplet state spectrum, indicating that the  $\pi^*$  density in the ring is comparable in the  $S_1$  and  $T_1$  states. As previously noticed,<sup>18,25</sup> the triplet state 8a frequency (1533  $\text{cm}^{-1}$ ) is significantly lowered by both ring and methyl deuteration, which is not the case in the ground state, radical cation, and  $S_1$  state spectra. Thus, a specific coupling occurs in the triplet state between the ring mode 8a and a motion involving the methyl groups. A strong coupling between the 8a and  $\nu_{\text{N-ring}}^s$  vibrations has been proposed,<sup>18,23,25</sup> favored by the low ring CC average bond order and a supposed high N-ring bond order. Unfortunately, the second 8a/ $\nu_{\text{N-ring}}^s$  mixed vibration could not be identified with certainty in the  $T_1$  state spectrum among the two possible lines at 1480 and 1435  $\text{cm}^{-1}$ .<sup>18</sup> The absence of this coupling effect in all molecular states but  $T_1$  is consistent with the fact that (i) in the radical cation the  $\nu_{\text{N-ring}}^s$  frequency is high (1420  $\text{cm}^{-1}$ ) but the 8a frequency remains much higher (1632  $\text{cm}^{-1}$ ), (ii) in the  $S_1$  state the 8a frequency is low (1515  $\text{cm}^{-1}$ ) but the  $\nu_{\text{N-ring}}^s$  mode remains much lower (1376  $\text{cm}^{-1}$ ),

and (iii) the ground-state molecule is characterized by both a high 8a frequency (1623 cm<sup>-1</sup>) and a low  $\nu_{\text{N-ring}}^{\text{s}}$  frequency (1345 cm<sup>-1</sup>). Though the S<sub>1</sub> and T<sub>1</sub> states have comparable 8a and 9a frequencies, they differ notably by their  $\nu_{\text{N-ring}}^{\text{s}}$  frequency. The weak value found for this mode in the S<sub>1</sub> state, close to the ground-state value, indicates that the single bond character of the N-ring bonds is preserved on going from S<sub>0</sub> to S<sub>1</sub>. Therefore, whereas in the T<sub>1</sub> state molecule partial conjugation of the nitrogen n electrons and ring  $\pi$  electrons leads to an extended quinoidal distortion with substantial double bond character of the N-ring bonds,<sup>18,23</sup> the structural distortion in the S<sub>1</sub> state is much more confined in the phenyl ring. In this respect, there is an obvious analogy between the TMB and TMPD S<sub>1</sub> state structures. The absence of coupling of the  $\nu_{\text{N-ring}}^{\text{s}}$  mode with the ring mode 8a (as observed in the case of the T<sub>1</sub> state) or with the CH<sub>3</sub> bending mode (as observed for the radical cation), well attested by its insensitivity to any deuteration, is consistent with the low  $\nu_{\text{N-ring}}^{\text{s}}$  frequency in the S<sub>1</sub> state. The resonance Raman activity of several CH<sub>2</sub> and CH<sub>3</sub> deformation modes of the alkyl groups is a common characteristic of the resonance Raman spectra of the S<sub>1</sub> state, T<sub>1</sub> state,<sup>18</sup> and radical cation.<sup>18</sup> It reveals that these CH<sub>2</sub> and CH<sub>3</sub> modes borrow some resonance Raman intensity to the  $\pi$  chromophore from their mechanical coupling with the low-frequency ring distortions 1 and 6a.

## Conclusion

The analysis of the picosecond resonance Raman spectra obtained for the lowest excited singlet state (S<sub>1</sub>) of the TMB and TMPD diamines for several isotopomers allowed us to establish a reliable vibrational assignment and to obtain structural information on this excited state. The molecular structure is mainly characterized by a notable lessening of the average ring CC bond strength with respect to the ground state structure, the electronic perturbation being essentially localized in the phenyl rings. Thus, contrary to what was previously found in the T<sub>1</sub> state and the radical cation, the N-ring bonds and, in the case of TMB, the inter-ring bond do not exhibit significant double bond character in the S<sub>1</sub> state. No quinoidal distortion is present and the anilino groups keep probably a conformation similar to that in the ground state.

**Acknowledgment.** The authors thank the Groupement de Recherche GDR 1017 from CNRS and the Centre d'Etudes et de Recherche Lasers et Applications (CERLA) for their help

in the development of this work. CERLA is supported by the Ministère chargé de la Recherche, Région Nord/Pas de Calais, and the Fonds Européen de Développement Economique des Régions (FEDER).

## References and Notes

- (1) Lewis, G. N.; Lipkin D. *J. Am. Chem. Soc.* **1942**, *64*, 2801.
- (2) Lesclaux, R.; Joussiot-Dubien, J. In *Organic Molecule Photophysics*; Birks, J. B., Ed.; Wiley-Interscience: London, 1973; Vol. 1, p 457.
- (3) Mattes, S. L.; Chanon, M. In *Organic Photochemistry*; Padwa, A., Ed.; M. Dekker: New York, 1983; Vol. 6, p 233.
- (4) Nakato, Y.; Yamamoto, N.; Tsubomura, H. *Bull. Chem. Soc. Jpn.* **1967**, *40*, 2480.
- (5) Ottolenghi, M. *Chem. Phys. Lett.* **1971**, *12*, 339.
- (6) Alchalal, A.; Ottolenghi, M. *Chem. Phys. Lett.* **1972**, *17*, 117.
- (7) Hirata, Y.; Mataga, N. *J. Phys. Chem.* **1983**, *87*, 1680.
- (8) Nakamura, S.; Kanamaru, N.; Nohara, S.; Nakamura, H.; Saito, Y.; Tanaka, J.; Sumitani, M.; Nakashima, N.; Yohihara, K. *Bull. Chem. Soc. Jpn.* **1984**, *57*, 145.
- (9) Hirata, Y.; Mataga, N. *J. Phys. Chem.* **1984**, *88*, 3091.
- (10) Hashimoto, S.; Thomas, J. K. *J. Phys. Chem.* **1984**, *88*, 4044.
- (11) Saito, T.; Haida, K.; Sano, M.; Hirata, Y.; Mataga, N. *J. Phys. Chem.* **1986**, *90*, 4017.
- (12) Hirata, Y.; Mori, Y.; Mataga, N. *Chem. Phys. Lett.* **1990**, *169*, 427.
- (13) Shimamori, H.; Tatsumi, Y. *J. Phys. Chem.* **1993**, *97*, 9408.
- (14) Shimamori, H.; Okuda, T. *J. Phys. Chem.* **1994**, *98*, 2576.
- (15) Shimamori, H.; Musasa, H. *J. Phys. Chem.* **1995**, *99*, 14359.
- (16) Hirata, Y.; Mataga, N. *Prog. React. Kinet.* **1993**, *18*, 273.
- (17) Isaka, H.; Abe, J.; Ohzeki, T.; Sakaino, Y.; Takahashi, H. *J. Mol. Struct.* **1988**, *178*, 101.
- (18) Poizat, O.; Bourkba, A.; Buntinx, G.; Deffontaine, A.; Bridoux, M. *J. Chem. Phys.* **1987**, *87*, 6379.
- (19) Brouwer, A. M. *J. Phys. Chem. A* **1997**, *101*, 3626.
- (20) Guichard, V.; Bourkba, A.; Poizat, O.; Buntinx, G. *J. Phys. Chem.* **1989**, *93*, 4429.
- (21) Boilet, L.; Buntinx, G.; Lapouge, C.; Lefumeux, C.; Poizat, O. *Phys. Chem. Chem. Phys.* **2003**, *5*, 834.
- (22) Yokoyama, K. *Chem. Phys. Lett.* **1982**, *92*, 93.
- (23) Abe, J.; Miyazaki, T.; Takahashi, H. *J. Chem. Phys.* **1989**, *178*, 2317.
- (24) Guichard, V.; Poizat, O.; Buntinx, G. *J. Phys. Chem.* **1989**, *93*, 4436.
- (25) Takahashi, H.; Werncke, W.; Pfeiffer, M.; Lau, A.; Johr, T. *Appl. Phys.* **1994**, *B59*, 403.
- (26) Guichard, V.; Bourkba, A.; Lautie, M. F.; Poizat, O. *Spectrochim. Acta* **1989**, *45*, 187.
- (27) Didierjean, C.; De Waele, V.; Buntinx, G.; Poizat, O. *Chem. Phys.* **1998**, *237*, 169.
- (28) Didierjean, C.; Buntinx, G.; Poizat, O. *J. Phys. Chem. A* **1998**, *102*, 7938.
- (29) Varsanyi, G. In *Assignments for vibrational spectra of seven hundreds benzene derivatives*; Lang, L., Ed.; Adam Hilger: London, 1974; Vol. I.
- (30) Wilson, E. B. *Phys. Rev.* **1934**, *45*, 706.
- (31) Hirata, Y.; Ichikawa, M.; Mataga, N. *J. Phys. Chem.* **1990**, *94*, 3872.